

Formation of Vacancies in Si- and Ge-based Clathrates: Role of Electron Localization and Symmetry Breaking

Amrita Bhattacharya,¹ Christian Carbogno,¹ Bodo Böhme,²
Michael Baitinger,² Yuri Grin,² and Matthias Scheffler^{1,3,4}

¹*Fritz Haber Institute of the Max Planck Society, Faradayweg 4-6, 14195 Berlin, Germany*

²*Max Planck Institute for Chemical Physics of Solids, Nöthnitzer Str. 40, 01187, Dresden, Germany*

³*Department of Chemistry and Biochemistry, University of California at Santa Barbara, CA 93106, USA*

⁴*Materials Department, University of California at Santa Barbara, CA 93106, USA*

(Dated: October 25, 2021)

The formation of framework vacancies in Si- and Ge-based type-I clathrates is studied as function of filling the cages with K and Ba atoms using density-functional theory. Our analysis reveals the relevance of structural disorder, geometric relaxation, electronic saturation, as well as vibrational and configurational entropy. In the Si clathrates we find that vacancies are unstable, but very differently, in Ge clathrates up to three vacancies per unit cell can be stabilized. This contrasting behavior is largely driven by the different energy gain on populating the electronic vacancy states, which originates from the different degree of localization of the valence orbitals of Si and Ge. This also actuates a qualitatively different atomic relaxation of the framework.

Clathrates are compounds with complex and large cage-like crystal structures (*hosts*) that can be filled with *guest* atoms or molecules (Fig. 1) [1]. Charge and heat transport in intermetallic clathrates has been studied intensively over the last decade [2], since filling would allow to increase their thermoelectric efficiency [3]. The uttermost majority of filled clathrates are, however, metallic [4–9] and thus unsuitable for this application in their pristine form. Nonetheless, puzzling exceptions exist, e.g., Ge_{46} filled with K: After decades of experiments [4–6], its semiconducting character was recently explained by a careful structure analysis [10], which revealed a high vacancy concentration ($\sim 4\%$). For this case, the puzzle appears to be resolved [11, 12]. However, high-quality synthesis and experimental analysis have remained challenging in this field. In particular, no fundamental understanding of the mechanism that determines vacancy formation and thus composition, structure, and electronic character upon filling exists. Therefore, these properties of clathrates are still unpredictable in practice.

The most prominent example are the isoelectronic Si and Ge type-I clathrates (see Fig. 1): These clathrates exhibit comparable properties in the unfilled case (cf. Tab. I and Ref. [13]), but behave remarkably different upon filling, e.g., with K or Ba guests. In the case of Si, the framework remains intact and metallic behavior (e.g. K_8Si_{46} [4–6] and $\text{Ba}_8\text{Si}_{46}$ [7–9]) results. In the case of Ge, vacancies \square occur in the host framework: In line with Zintl’s concept, a heavily doped semiconductor $\text{K}_8\text{Ge}_{44}\square_2$ featuring two framework vacancies was found experimentally for monovalent K guests [6, 10]. For divalent Ba guests, however, experiments [14, 15] found a metallic $\text{Ba}_8\text{Ge}_{43}\square_3$ compound with three vacancies, but not four, as expected from the increased Ba valence. In this work, we present a quantitatively reliable theoretical prediction of the structure, vacancy concentration (composition), electronic character, and thermodynamic sta-

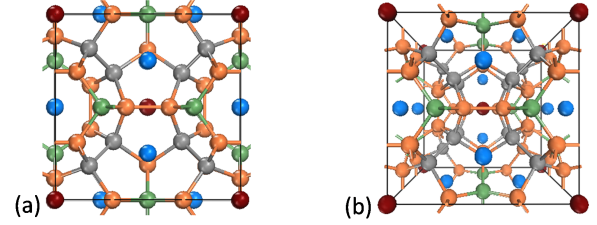


FIG. 1. Crystal structure (space group $Pm\bar{3}n$) of type-I clathrates [2]. Colors denote the Wyckoff sites for the host (6c green, 16i grey, and 24k orange) and the guest atoms (2a red, 6d blue).

bility for these binary K/Ba-Si/Ge systems. These findings explain the existing experimental results and provide an atomistic mechanism for the contrasting behavior of Si and Ge clathrates.

Density-functional theory (DFT) [16, 17] calculations were performed with *FHI-aims* [18, 19], an all-electron, full-potential electronic-structure code that uses numeric, atom-centered basis sets. Numerical settings were chosen to achieve a convergence in energy differences better than 10^{-3} eV/atom (see Suppl. Mat.). To ensure that our findings are independent from the chosen treatment for exchange and correlation (xc), we compare how various xc-functionals describe both the equilibrium properties of the empty F_{46} clathrates ($F = \text{Si, Ge}$) and the charged vacancy [20]. Its formation energy is calculated using the total energy difference [21]

$$E_{\square}^q = E(F_{45}\square_1^q) - E(F_{46}) + \frac{E(F_2^{\text{Dia}})}{2} + q(\mu_e - \text{VBM}) \quad (1)$$

between the defective framework $E(F_{45}\square_1^q)$ with charge q and the pristine clathrate $E(F_{46})$. The diamond phase $E(F_2^{\text{Dia}})$ and the electron chemical potential μ_e relative to the valence band maximum VBM act as ther-

	Si ₄₆						Ge ₄₆					
	a_0	E_c	ϵ_g	E_{\square}^0	$I_{0/4-}$		a_0	E_c	ϵ_g	E_{\square}^0	$I_{0/4-}$	
LDA	10.11	3.8	1.14	3.33	0.93		10.49	2.2	1.25	2.97	0.60	
PBEsol	10.17	3.4	1.21	3.35	0.95		10.59	1.9	1.23	2.92	0.58	
PBE	10.23	2.7	1.33	3.43	1.10		10.74	1.5	1.12	2.80	0.57	
RPBE	10.30	2.0	1.43	3.50	1.08		10.84	1.0	1.09	2.77	0.58	
HSE06	10.18	3.4	1.90	3.85	1.48		10.62	1.7	1.89	3.32	0.95	

TABLE I. Properties of empty Si₄₆ and Ge₄₆ clathrates computed in the 46 atom unit cell for various xc-functional: Lattice parameter a_0 (Å), cohesive energy E_c (eV), Kohn-Sham band gap ϵ_g (eV), neutral vacancy formation energy E_{\square}^0 (eV), and charge transition level $I_{0/4-}$ with respect to the top of the valence band. The atomic chemical potential (for E_c and E_{\square}^0) is that of the diamond structure.

modynamic reservoirs. The VBM of the defective and of the pristine clathrate (VBM^{Pr}) are referenced using the core level shift ΔV between $F_{45}\square_1^q$ and F_{46} : $\text{VBM} = \text{VBM}^{\text{Pr}} + \Delta V$. Charge transition levels $I_{q/q'}$, which quantify the energy involved in charging the vacancy [21], are computed using the value of μ_e at which $F_{45}\square_1^{q'}$ and $F_{45}\square_1^q$ are in equilibrium

$$I_{q/q'} = \frac{E(F_{45}\square_1^{q'}) - E(F_{45}\square_1^q)}{q - q'} + \text{VBM}. \quad (2)$$

For the local-density approximation (LDA) [22]), variants of the generalized gradient approximation (PBE [23], PBEsol [24], RPBE [25]), and the computationally more involved HSE06 functional [26] that incorporates a fraction of exact exchange, Tab. I lists the lattice parameter a_0 , cohesive energy E_c , and band gap ϵ_g for the empty F_{46} clathrates as well as the formation energy for a neutral vacancy E_{\square}^0 at the 6c site and its transition level $I_{0/4-}$, which characterizes the typical charge state in these clathrates (see below). We find the typical over/underbinding of LDA/PBE for a_0 and E_c , whereby PBEsol gives results similar to HSE06 (differences are $< 0.5\%$ for a_0 and < 5 meV/atom for E_c). Deviations in the vacancy formation energies E_{\square}^0 and transition levels $I_{0/4-}$ are, however, noticeable. In the following, PBEsol was thus employed in the structural search. We explicitly checked that the relative energetic ordering of the thereby identified compositions is retained with HSE06 (see Suppl. Mat.).

To determine the stable vacancy concentrations in Si and Ge frameworks filled with K or Ba guests (G), we have first identified the energetically favorable configurations for all compositions $G_n F_{46-y}\square_y$ with $n \in [0, 8]$ guests and $y \in [0, 4]$ vacancies using an iterative strategy that required ~ 1400 full structural relaxations: Starting from the completely filled clathrate, we have first identified the most favorable vacancy sites by scanning

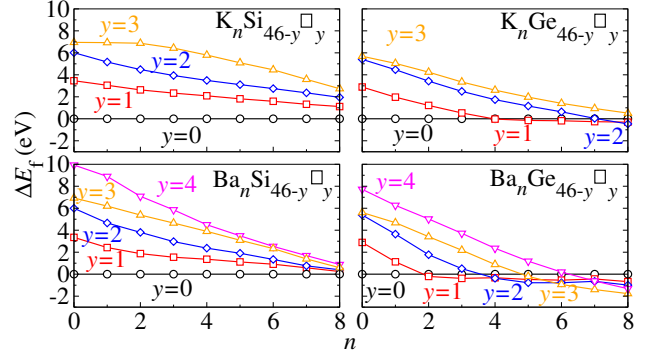


FIG. 2. Calculated (DFT-PBEsol) formation-energy difference $\Delta E_f = E_f(G_n F_{46-y}\square_y) - E_f(G_n F_{46})$ as function of the filling n with K and Ba guests.

over all possible framework positions. Then, we stepwise removed guests from the compositions with fully occupied and defective framework, again scanning over all available guest sites. For any subsequent composition, we retained the already identified guest and vacancy sites and thus limited the scanning to the remaining available positions. Eventually, we computed the formation energies of these compositions using the stoichiometrically balanced energy difference

$$E_f(n, y) = E(G_n F_{46-y}\square_y) - \frac{46 - y - n \cdot x}{2} \cdot E(F_2^{\text{Dia}}) - n \cdot E(G_1 F_x) \quad (3)$$

between filled and/or defective clathrate $E(G_n F_{46-y}\square_y)$ and the reservoirs for framework F and guest atoms G , i.e., F_2^{Dia} and the thermodynamically stable neighboring phases $G_1 F_x$ (K_4Si_4 [27], BaSi_2 [28], K_4Ge_4 [29], and $\text{Ba}_6\text{Ge}_{25}$ [30]). As the formation energy differences in Fig. 2 show, vacancy formation is always energetically unfavorable in Si clathrates by $\Delta E_f > 0.3$ eV/vacancy, but not in Ge clathrates: In the fully filled case, di-vacancy ($\text{K}_8\text{Ge}_{44}\square_2$) and tri-vacancy formation ($\text{Ba}_8\text{Ge}_{43}\square_3$) are energetically favorable by $\Delta E_f < -0.1$ eV/vacancy; partial filling ($n < 8$) makes smaller vacancy concentrations preferable [31].

Fig. 2 also reveals that vacancy formation energies generally decrease with increasing filling, so that the question arises, if the fully filled clathrates identified as stable at 0 K are also the most stable ones at finite temperatures. To clarify, we have computed their thermodynamic stability by accounting for configuration entropy and vibrational free energies (see Suppl. Mat.). As shown in Fig. 3, we find that the compositions discussed above (K_8Si_{46} , $\text{K}_8\text{Ge}_{44}\square_2$, $\text{Ba}_8\text{Si}_{46}$, $\text{Ba}_8\text{Ge}_{43}\square_3$) are also stable at room temperature. Interestingly, we find that vacancies in the K-filled Ge clathrate become less favorable with increasing temperature, which reflects that their formation is energetically favorable but entropically adverse due to the harder vibrations present in defective

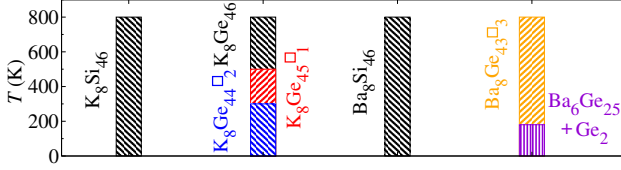


FIG. 3. Most favorable compositions of K/Ba-filled Si/Ge clathrates as a function of temperature T computed at the DFT-PBESol level.

frameworks (see Suppl. Mat.). Since this compound is typically synthesized at temperatures > 600 K [4–6, 10], this explains reports of less than two vacancies per unit cell [32]. Accordingly, our calculations correctly reproduce the trends in formation and phase stability for all compositions observed experimentally [5, 7, 10], including the eutectoid decomposition of $\text{Ba}_8\text{Ge}_{43}\square_3$ [15].

Furthermore, our calculations consistently reproduce the electronic character found for these compositions experimentally: The guests donate electrons to the framework, which leads to a partial filling of the conduction band and thus to a metallic electronic structure in the stable, vacancy-free Si clathrates (8 and 16 charge carriers/f.u. for K and Ba with $n = 8$). Conversely, the vacancies in the Ge framework accommodate up to four surplus electrons each, as suggested by qualitative models [11, 12]. Due to the completely occupied vacancy states, $\text{K}_8\text{Ge}_{44}\square_2$ is a semiconductor with a band gap of 0.18/0.28 eV (PBESol/HSE06). Similarly, all vacancy states are occupied in $\text{Ba}_8\text{Ge}_{43}\square_3$, but the four additional electrons accommodated in the conduction band lead to a metallic electronic structure.

Our studies confirm that filled Si- and Ge-based clathrates behave remarkably even qualitatively differently in spite of their isoelectronicity. Fig. 2 also suggests the mechanism that stabilizes vacancies in Ge, but not in Si: In Ge, the slope $\partial\Delta E_f(n, y)/\partial n$ changes significantly whenever the number of guest atoms n matches $n = 4y/z$ (z is the valency of the guest cation), e.g., for $\text{K}_4\text{Ge}_{45}\square_1$ or $\text{Ba}_4\text{Ge}_{44}\square_2$. Regardless of the guests' species, the Ge compositions meeting this condition are energetically favorable and are the only ones that exhibit semiconducting character. Conversely, such distinct changes in the slope are not observed in Si, for which $\partial\Delta E_f(n, y)/\partial n$ is almost independent on the number of guests. Since $\Delta E_f(n, y)$ is defined as the energy difference between the defective and the completely occupied host framework, its slope $\partial\Delta E_f(n, y)/\partial n$ is related to the energy gain stemming from charging the vacancy.

In more detail, this mechanism can be rationalized by inspecting the electronic structure of these defected clathrates: As sketched in Fig. 4, the guests lose their valence electrons in state ϵ_G to the energetically lower lying conduction band minimum ϵ_{CBm} or – if available – to the vacancy states $I_{q/q'}$ in the band gap. The

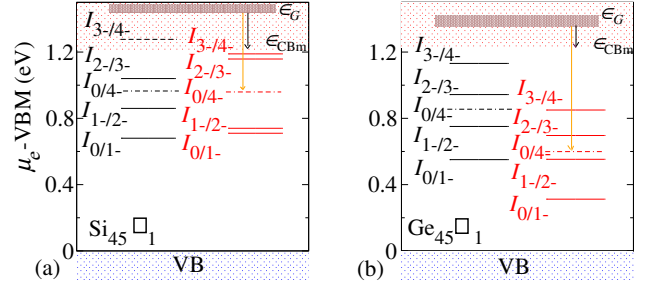


FIG. 4. Calculated (DFT-PBESol) charge transition levels $I_{q/q'}$ of (a) $\text{Si}_{45}\square_1$ and (b) $\text{Ge}_{45}\square_1$ with the unrelaxed (black) and fully relaxed (red) geometry. Schematically, the positions of the guest levels ϵ_G in the conduction band are drawn as well to highlight the energy gains E_{CBm} and E_{\square} associated with electron transfer from ϵ_G to the conduction band minimum ϵ_{CBm} (black arrow) and to the vacancy's ionization level $I_{0/4-}$ (orange arrow).

respective energy gains are $E_{\text{CBm}} = \epsilon_G - \epsilon_{\text{CBm}}$ and $E_{q/q'} = \epsilon_G - I_{q/q'}$. In first order approximation, their difference $\Delta E_{q/q'} = E_{\text{CBm}} - E_{q/q'}$ determines the slope $\partial\Delta E_f(n, y)/\partial n$ for $n \leq 4y/z$. Please note that by definition $\Delta E_{q/q'}$ is not particularly sensitive on the guests' species (see Suppl. Mat.), but is predominantly determined by the host. Surprisingly, this reveals that the contrasting tendency to suppress/form vacancies in Si and Ge frameworks is largely controlled by the charge transition levels of their vacancies. Indeed, Fig. 2 and 4 consistently show that both $\partial\Delta E_f(n, y)/\partial n$ and $\Delta E_{q/q'}$ are much smaller in Si than in Ge. Accordingly, the different properties of a single vacancy in guest-free $\text{Si}_{45}\square_1$ and $\text{Ge}_{45}\square_1$ also allow to rationalize the underlying mechanism: Quantitatively, the energetic cost E_{\square}^0 to create a neutral vacancy is indeed slightly higher by ≈ 0.4 eV in Si (cf. Tab. I); the energetic gain $\Delta E_{0/4-} = -4(\epsilon_{\text{CBm}} - I_{0/4-})$ obtained from fully charging the vacancy is, however, distinctly larger in Ge by ≈ -1.2 eV and thus exceeds the cost of creating a vacancy – but only if geometric relaxations are accounted for (cf. Fig. 4). In the unrelaxed case, the charge transition levels $I_{q/q'}$ show only slight quantitative differences for Si and Ge, but the exact same qualitative behavior. Upon geometry relaxation, however, the charge transition levels in Si form energetically almost degenerate, zero-U [33] pairs $I_{0/1-}$ and $I_{1-/2-}$ as well as $I_{2-/3-}$ and $I_{3-/4-}$, whereby $I_{0/4-}$ is virtually unaltered. Conversely, the individual levels including $I_{0/4-}$ undergo distinct shifts to lower energies in Ge, which explains the large overall energy gain $\Delta E_{q/q'}$. This demonstrates that the contrasting behavior of Si and Ge clathrates is neither driven by guest-host interactions nor by the different cost of creating neutral vacancies, but is predominantly determined by electron transfer processes upon charging.

These electron transfer processes result from the different character of the Si and Ge transition levels, which

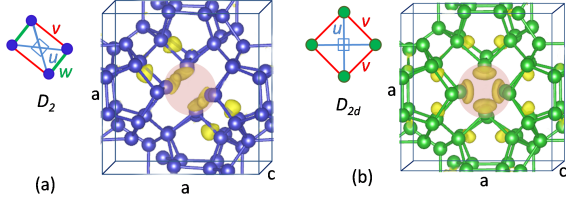


FIG. 5. Calculated (DFT-PBEsol) geometries of the relaxed $F_{45}\square_1^{4-}$ vacancy in empty (a) Si and (b) Ge clathrates. The isosurface (isovalue $0.015 \text{ e}\text{\AA}^{-3}$) of the charge density difference with respect to the uncharged system $F_{45}\square_1^0$ is shown and the vacancy region is highlighted.

arise from different geometric distortions. Qualitatively, this is reflected in the electron distribution around the vacancy (Fig. 5). Quantitatively, we use the interatomic distances u , v , and w between the vacancy's neighbors (cf. Fig. 5 and [34, 35]) and the lattice parameter ratio c/a to characterize the local and global symmetry. In the unrelaxed case ($c/a = 1$), the neutral vacancy exhibits a global D_{2d} symmetry with nearest neighbor distances u (3.90 Å in Si, 4.07 Å in Ge) and $v = w$ (3.86 Å in Si, 4.02 Å in Ge). In the case of $\text{Ge}_{45}\square_1$, the local D_{2d} symmetry ($u = 3.15 \text{ Å}$, $v = w = 3.39 \text{ Å}$) and the cubic lattice ($c/a \leq 1.01$) are essentially retained when relaxing the fully charged vacancy. Conversely, we find that the fully charged Si vacancy features a local D_2 symmetry ($u = 2.98 \text{ Å}$, $v = 3.55 \text{ Å}$) with a drastically shortened pair of distances $w = 3.07 \text{ Å}$. Also, a **global** break in lattice symmetry (tilting $\gamma = 92^\circ$ and $c/a = 1.02$) occurs, which results in a splitting of the charge density around the vacancy in two distinct lobes. The same qualitative behavior also occurs in filled clathrates (see Suppl. Mat.). Please note that contrasting local relaxation patterns have been reported for the vacancy in the respective Si and Ge diamond phases [34, 35], too, but not a global symmetry break as in this case.

This peculiar and contrasting relaxation behavior of vacancies in clathrates can be attributed to the fact that the $3sp^3$ valence orbitals in Si_{46} are spatially more localized than the $4sp^3$ orbitals in Ge_{46} . Accordingly, the Si framework is more rigid, which results in almost twice as high phonon frequencies (see Suppl. Mat.). In turn, this allows local atomic and global lattice degrees of freedom to decouple and to break the symmetry independently. Thus, vacancy creation in empty Si_{46} leads to pairs of energetically unfavorable, spatially localized non-interacting states ($I_{0/1-} \approx I_{1-/2-}$ and $I_{2-/3-} \approx I_{3-/4-}$, Fig. 4). Conversely, the charged vacancy in $\text{Ge}_{45}\square_1$ forms a bulk state that retains the global symmetry and spans the vacancy in spite of the large nearest neighbor distances. Simultaneously, this lowers the charge transition levels upon relaxation. This interpretation in terms of localization of valence orbitals is substantiated by the volume dependence of the charge transition levels shown

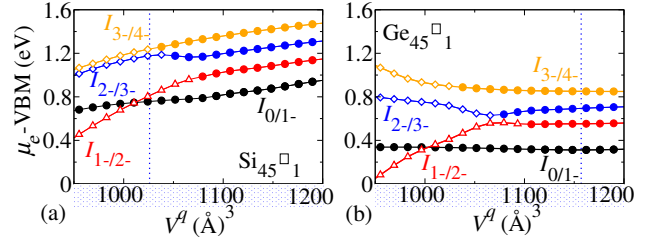


FIG. 6. Calculated (DFT-PBEsol) charge transition levels $I_{q/q'}$ of (a) $\text{Si}_{45}\square_1$ and (b) $\text{Ge}_{45}\square_1$ as a function of unit cell volume V^q with vacancies in charge state q (● corresponds to a D_{2d} symmetry, ◇ to D_2 and △ denotes the situation when q and q' differ in symmetry). The vertical lines denote the scenarios at the equilibrium-volume.

in Fig. 6. For all charge states q , we have computed E_{\square}^q at different volumes in **both** the lattice configurations with a local D_2 and D_{2d} symmetry, i.e., for the different c/a ratios and tiltings γ discussed before and listed in the Suppl. Mat. The energetically most favorable E_{\square}^q is used to determine the transition levels $I_{q/q'}$. Expanding $\text{Si}_{45}\square_1$ and thus enforcing an increased delocalization results in D_{2d} -type charge transition levels. Conversely, lattice compression (enforced localization) leads to D_2 -type levels in $\text{Ge}_{45}\square_1$ (Fig. 6). This shows that the discussed effects, which are driven by global and local symmetry breaking, are inherently related to the relationship between nearest neighbor distance (more than $\sim 10\%$ larger in clathrates than in the respective diamond structures) and valence orbital localization.

In summary, this work shows that vacancy formation is energetically not favorable in Si clathrates, neither for K nor for Ba filling. Conversely, two vacancies per unit cell are formed in Ge clathrates fully filled with K, and three vacancies in the case of Ba. In turn, this determines the different electronic character of these compounds. Regardless of the guest, the decisive energetic contribution for this contrasting behavior does not stem from the guests-host interaction or the formation of the neutral vacancy, but from its charging. The occurring electron transfer processes are quantitatively and qualitatively different in Si and Ge, since their different degree of valence orbital localization leads to contrasting structural relaxation patterns (global and local symmetry breaking). The stoichiometry, thermodynamic stability, and electronic structure of these materials is thus determined by this microscopic mechanism, which arises from the large ratio of nearest neighbor distance and valence orbital localization. Accordingly, our study suggests that this mechanism can be influential also in other materials with elongated bonds, e.g., skutterudites [36], Heusler alloys [37], boroncarbides [38], and perovskites [39]. Also in these cases, vacancy formation and its influence on structural and electronic properties are lively topics of research [40–43].

The authors thank Sergey Levchenko and Patrick Rinke for many fruitful discussions. The work was partially funded by Einstein foundation (project ETERNAL) and the European Union's Horizon 2020 research and innovation program under grant agreement no. 676580, The Novel Materials Discovery (NOMAD) Laboratory, a European Center of Excellence.

-
- [1] T. Takabatake, K. Suekuni, T. Nakayama, and E. Kaneshita, *Rev. Mod. Phys.* **86**, 669 (2014).
 - [2] G. S. Nolas, ed., *The Physics and Chemistry of Inorganic Clathrates* (Springer Dordrecht, 2014).
 - [3] M. Christensen, S. Johnsen, and B. B. Iversen, *Dalton Trans.* **39**, 978 (2010).
 - [4] C. Cros, M. Pouchard, and P. Hagenmuller, *J. Solid State Chem.* **2**, 570 (1970).
 - [5] G. K. Ramachandran and P. F. McMillan, *J. Solid State Chem.* **154**, 626 (2000).
 - [6] H. G. von Schnering, J. Llanos, K. Peters, M. Baitinger, Y. Grin, and R. Nesper, *Z. Kristallogr. NCS* **226**, 9 (2011).
 - [7] S. Yamanaka, E. Enishi, H. Fukuoka, and M. Yasukawa, *Inorg. Chem.* **39**, 56 (2000).
 - [8] R. Lortz, R. Viennois, A. Petrovic, Y. Wang, P. Toulemonde, C. Meingast, M. M. Koza, H. Mutka, A. Bossak, and A. San Miguel, *Phys. Rev. B* **77**, 224507 (2008).
 - [9] R. Castillo, W. Schnelle, M. Bobnar, U. Burkhardt, B. Böhme, M. Baitinger, U. Schwarz, and Y. Grin, *Z. Anorg. Allg. Chem.* **641**, 206 (2015).
 - [10] M. Beekman and G. S. Nolas, *Int. J. Appl. Ceram. Technol.* **4**, 332 (2007).
 - [11] H. G. von Schnering, *Nova Acta Leopold.* **59**, 165 (1985).
 - [12] H. G. von Schnering, *Bol. Soc. Chil. Quim.* **33**, 41 (1988).
 - [13] D. Connetable, *Phys. Rev. B* **82**, 075209 (2010).
 - [14] W. Carrillo-Cabrera, S. Budnyk, Y. Prots, and Y. Grin, *Z. Anorg. Allg. Chem.* **630**, 2267 (2004).
 - [15] U. Aydemir, C. Candolfi, H. Borrmann, M. Baitinger, A. Ormeci, W. Carrillo-Cabrera, C. Chubilleau, B. Lenoir, A. Dauscher, N. Oeschler, F. Steglich, and Y. Grin, *Dalton Trans.* **39**, 1078 (2010).
 - [16] P. Hohenberg and W. Kohn, *Phys. Rev.* **136**, B864 (1964).
 - [17] W. Kohn and L. J. Sham, *Phys. Rev.* **140**, A1133 (1965).
 - [18] V. Blum, R. Gehrke, F. Hanke, P. Havu, V. Havu, X. Ren, K. Reuter, and M. Scheffler, *Comput. Phys. Commun.* **180**, 2175 (2009).
 - [19] F. Knuth, C. Carbogno, V. Atalla, V. Blum, and M. Scheffler, *Comput. Phys. Commun.* **190**, 33 (2015).
 - [20] C. W. Weinert and M. Scheffler, *Phys. Rev. Lett.* **58**, 1456 (1987).
 - [21] C. Freysoldt, B. Grabowski, T. Hickel, J. Neugebauer, G. Kresse, A. Janotti, and C. G. Van de Walle, *Rev. Mod. Phys.* **86**, 253 (2014).
 - [22] J. P. Perdew and Y. Wang, *Phys. Rev. B* **45**, 13244 (1992).
 - [23] J. P. Perdew, K. Burke, and M. Ernzerhof, *Phys. Rev. Lett.* **77**, 3865 (1996).
 - [24] J. P. Perdew, A. Ruzsinszky, G. I. Csonka, O. A. Vydrov, G. E. Scuseria, L. A. Constantin, X. Zhou, and K. Burke, *Phys. Rev. Lett.* **100**, 136406 (2008).
 - [25] B. Hammer, L. B. Hansen, and J. K. Nørskov, *Phys. Rev. B* **59**, 7413 (1999).
 - [26] A. V. Krukau, O. A. Vydrov, A. F. Izmaylov, and G. E. Scuseria, *J. Chem. Phys.* **125**, 224106 (2006).
 - [27] H. G. von Schnering, M. Schwarz, J.-H. Chang, P. K., E.-M. Peters, and R. Nesper, *Z. Kristallogr. NCS* **220**, 525 (2005).
 - [28] T. Goebel, Y. Prots, and F. Haarmann, *Z. Kristallogr. NCS* **224**, 7 (2009).
 - [29] H. G. von Schnering, J. Llanos, J.-H. Chang, K. Peters, E.-M. Peters, and R. Nesper, *Z. Kristallogr. NCS* **220**, 324 (2005).
 - [30] W. Carrillo-Cabrera, J. Curda, von Schnering, H. G., S. Paschen, and Y. Grin, *Z. Kristallogr. NCS* **215**, 207 (2000).
 - [31] In all cases, the first two vacancies are most favorable at 6c, the third and fourth at 24k positions. However, taking into account superstructure formation in $\text{Ba}_8\text{Ge}_{43}\square_3$ [15], the experimentally reported vacancy configuration ($2 \times 2 \times 2$ superstructure; space group $Ia\bar{3}d$) is found to be slightly more stable by 0.05 (PBEsol) and 0.07 (HSE06) eV/f.u..
 - [32] J. Llanos, Ph.D. thesis, Stuttgart University (1984).
 - [33] U is calculated from Eq. 1 using the expression $U = E_{\square}^{q+2}(\mu_e = 0) + E_{\square}^q(\mu_e = 0) - 2E_{\square}^{q+1}(\mu_e = 0)$.
 - [34] G. A. Baraff, E. O. Kane, and M. Schlüter, *Phys. Rev. B* **21**, 5662 (1980).
 - [35] A. Fazzio, A. Janotti, A. J. R. da Silva, and R. Mota, *Phys. Rev. B* **61**, R2401 (2000).
 - [36] G. Li, Q. An, W. Li, I. William A. Goddard, P. Zhai, Q. Zhang, and G. J. Snyder, *Chemistry of Materials* **27**, 6329 (2015), <http://dx.doi.org/10.1021/acs.chemmater.5b02268>.
 - [37] L. Offernes, P. Ravindran, and A. Kjekshus, *Journal of Alloys and Compounds* **439**, 37 (2007).
 - [38] M. M. Balakrishnarajan, P. D. Pancharatna, and R. Hoffmann, *New J. Chem.* **31**, 473 (2007).
 - [39] M. Johnsson and P. Lemmens, in *Handbook of Magnetism and Advanced Magnetic Materials* (John Wiley and Sons Ltd, 2007).
 - [40] G. P. Meisner, D. T. Morelli, S. Hu, J. Yang, and C. Uher, *Phys. Rev. Lett.* **80**, 3551 (1998).
 - [41] I. Galanakis, E. Şaşıoğlu, S. Blügel, and K. Özdoğan, *Phys. Rev. B* **90**, 064408 (2014).
 - [42] R. Schmechel and H. Werheit, *Journal of Physics: Condensed Matter* **11**, 6803 (1999).
 - [43] R.-A. Eichel, *Phys. Chem. Chem. Phys.* **13**, 368 (2011).